

The effect of hot rolling and coiling temperature on microstructure and texture of ferritic stainless steel

A. Kisko, A. Kaijalainen, L. Kurtti, S. Kodukula, T. Ylimäinen

The effect of hot rolling and coiling temperature on microstructure and texture of stabilized high-Cr ferritic stainless steel was investigated. The steel sheets were hot-rolled at a hot rolling mill with three finishing rolling and two coiling temperatures. The microstructure and texture of steel were characterized at the surface and centreline using the electron backscatter diffraction technique. Microstructure studies showed that at the surface high finish rolling temperature promoted the formations of substructure (low-angle boundaries) and recrystallized grains instead of deformed grains. At the centreline, the low finishing hot rolling temperature increased the tendency of deformed structure and decreased the tendency of recrystallized structure. Lowering the coiling temperature, promoted substructure and decreased the tendency of deformed grains. It was observed that at the surface layer of the investigated materials contains $\sim\{112\}<111>$, $\sim\{110\}<112>$ and $\sim\{011\}<110>$ and shear texture components and at the centreline mainly $\sim\{554\}<225>$, $\sim\{001\}<110>$, $\sim\{112\}<110>$ and $\sim\{112\}<131>$ texture components. A decrease in finish rolling and coiling temperature strengthens the texture intensities at the subsurface. At the centreline, lower finish rolling and coiling temperatures sharpened the α - and γ - fibres and texture.

KEYWORDS: FERRITIC STAINLESS STEEL, HOT ROLLING, MICROSTRUCTURE, TEXTURE, GRAIN SIZE, ELECTRON BACKSCATTER DIFFRACTION;

INTRODUCTION

Ferritic stainless steels (FSS), containing over 17% Cr, are very promising steel for several applications. The low Ni and Mo concentrations, together with Cu alloying and high-Cr content ensure good corrosion resistance, even comparable to that of the commonly used austenitic stainless steel grade such as AISI 304, but with much lower alloying costs. Other key properties for high-Cr ferritic stainless steels are heat resistance and good combinations of mechanical properties [1]. Likewise, the high-Cr ferritic stainless steels are used in wide-scale varying from kitchen appliances, building materials, and different mobile components. Indeed, one of the most demanding components is the exhaust system where high-Cr FSSs have been replacing conventional cast iron as the most commonly used material [2,3]. The processing of those highly demanding applications need often deep drawability. Unfortunately, ferritic stainless steels are prone to the surface defect called ridging [4]. Riding

Anna Kisko, Antti Kaijalainen
University of Oulu, Finland

Lauri Kurtti, Suresh Kodukula, Tapani Ylimäinen
Outokumpu Stainless Oy, Finland

defects appear as corrugations parallel to the rolling direction as they arise after the deep drawing process to the steel sheet. The only way to remove ridges from the steel sheet is by polishing, but the additional process step is not desirable. Hence, the prevention of the ridges is extremely important.

The solidification structure of the ferritic stainless steels may consist of columnar grains and during re-crystallization, they will transform into bands or similarly oriented grains. Orientation of the grains may remain until the final steel sheet. As these grains have different plastic anisotropies compared with the matrix, ridging may occur since ridging defects are caused by differences in the plastic anisotropies of grains and heterogeneities in the texture structure [5]. The hot rolling stage effects to the texture of the final steel sheet.

During cold rolling, the hot band textures might even sharpen slightly as the texture of the final product is inherited from the hot band [6,7]. Since stabilized FSS does not undergo an austenite-ferrite transformation, hot rolling or hot band annealing are the only ways to affect to the formed texture. At the hot rolling stage, the temperature profile and the strained state varies through-thickness of the sheet resulting shear deformation at the subsurface and plain strain deformation at the centreline [8]. A higher amount of stored energy, caused by deformation, is stored in a colder surface leading to partial recrystallization, whereas the temperature in centre layer is high enough for dynamic recovery to occur. This leads to a pancake-like microstructure in centreline. The desirable texture in stabilized FSS is closely related to the γ -fibre texture [9]. Hence, the understanding of the evolution of the hot rolling and coiling temperature to the formed micro-structure and texture is extremely important.

In this study the effect of the hot rolling finishing and coiling temperature to the formed microstructure, grain size and texture were studied. Also, the changes in the hot rolling finishing and coiling temperatures to the formed structure and texture at the subsurface and centreline are discussed.

EXPERIMENTAL PROCEDURE

The investigated material is EN 1.4509 from Outokumpu Stainless Oy (Tornio, Finland) production site/pilot scale rolling mill. The chemical composition is Fe-<0.05C-17.6Cr-0.4Si-<0.5(Ti+Nb) (in wt.%). Materials finish rolling temperature (FRT) and coiling temperature (CT) were varied. Each sample was coded according to its finish rolling temperature (low, middle or high) and the coiling temperature (low or high). Therefore, six hot band variations of the 3 mm thickness are investigated.

Microstructural examination and microtexture analysis were performed using field emission scanning electron microscope (JEOL-JSM-7900F FESEM) together with electron backscatter diffraction (EBSD) device (Oxford Instrument HKL, Aztec and Channel5 software). The EBSD measurements were conducted using accelerating voltage of 20 kV, working distance of 16-21 mm and step size of 0.5 μ m. The characterization was performed for RD-ND (rolling-normal directions) at the subsurface and centreline of 1200 μ m x 800 μ m area.

RESULTS AND DISCUSSION

Fig. 1 shows the inverse pole figure (IPF) maps obtained by EBSD for the studied steel samples from the surface and centreline. The subsurface is located at the top of the surface of the sample's images. It is seen that the FRT and CT affect the formed microstructure, sub-boundaries, and the degree of dynamic restoration. The microstructural variations are visible between the subsurface and centreline samples. At low FRT the microstructure is still mostly in a deformed state whereas at high FRT the sample is dynamically recovered. The number of low-angle grain boundaries decreases significantly as the FRT increases. The corresponding trend is seen with the coiling temperature.

The studied ferritic stainless steels hot bands have quite a typical hot deformed structure since after hot rolling stabilized FSSs usually has a strong texture gradient through the thickness (Fig. 1). From Fig. 1 can be seen that at the subsurface layers tiny grains are recrystallized along RD. The grain size seems to increase gradually through

the thickness and their shape changes from the equiaxed towards the pancaked structure. The highly elongated grains are visible of about 200-400 μm from the sample's edge. Hence, highly elongated grains with a length over 600 μm along to the rolling direction are seen both at the surface and centreline.

Generally, the highly deformed i.e. pancaked grains contained different amounts of low-angle grain boundaries. In some of the deformed grains were numerous low-angle grain boundaries aligned at 35° to the rolling direction. These aligned boundaries are also called in the literature as in-grain shear bands [10,11], which refer to recovered grains. More in-grain shear bands were detected in the specimens with low or middle than in high FRT samples. Low CT also increased the amount of in-grain shear bands, which may be due to the slight static recovery taking place during high CT i.e. slow cooling. Hence, the formation of the in-grain shear band required relatively low temperatures, which is supported by the literature [10]. Lowering the FRT from high, middle to low led to a significant flattened structure and increase the number of low-angle grain

boundaries.

In the further processing steps, in-grain shear bands offer nucleation sites for static recrystallization. $<111>/\text{ND}$ grains belonging to γ -fibre nucleates to these in the in-grain shear bands. In order to obtain good final product properties, the presence of in-grain shear bands should be promoted. This can be done by decreasing CT.

It is seen that the microstructure of the hot band subsurface has the orientations of $<001>/\text{ND}$ and $<111>/\text{ND}$ as shown in red and purple (Fig. 1). This so-called shear texture is a result of shear deformation at the surface layer and consists mainly of Goss texture with the $\{011\} <100>$ orientation.

At the centreline, the microstructure is highly pancaked. The low-angle grain boundaries are visible, which might refer to the recovered grain structure. The highly elongated grains with 101 orientations are shown in green (Fig. 1). The α -fibre texture is formed due to the strain deformation conditions and is dominated by the $\{001\} <110>$ orientation.

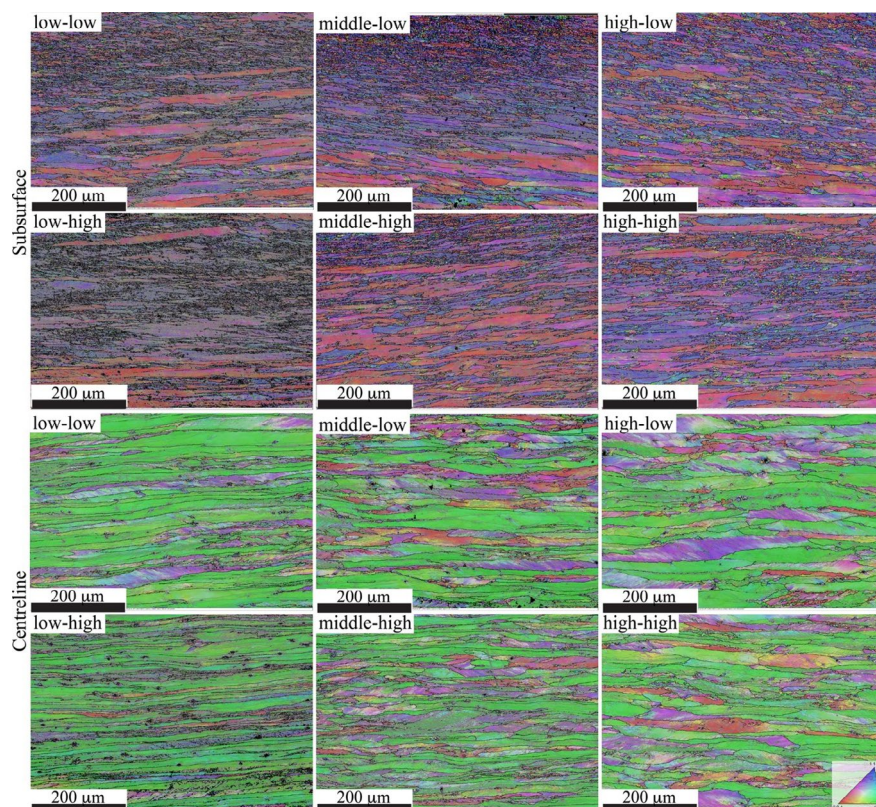


Fig.1 - Inverse pole figure maps (coloured of RD direction) of RD-ND section of the hot bands obtained by EBSD. The black-coloured grain boundaries have misorientation higher than 15° and the grey coloured grain boundaries between $2.5 - 15^\circ$.

The recrystallized, recovered and deformed structure fractions for the studied steels obtained from EBSD data are shown in Table 1 and Fig. 2. The amount of deformed structure decreases as FRT and CT increase. Low FRT enables higher stored energy in the structure promoting further recrystallization during annealing. As FRT and CT increase, recovered and recrystallized fractions of the samples increase in many samples. As discussed earlier, in-grain shear bands refer to the recovered structure, which fraction is higher at the centreline than in the surface. At the surface, more recrystallized grains are detected as tiny, recrystallized grains appear near the surface.

Typically, FRT affects to the recrystallization rate more at the subsurface than in the centreline as increasing FRT from low to high, recrystallized fraction increased from

4.7% to 19.5% in high CT and from 5.6% to 19.0% in low CT. This is due to the heat conductivity during cooling which enables faster cooling at the subsurface than in centreline. The same phenomenon is detected for the recovered structure.

The finish hot rolling temperature effects to the stored energy of the ferritic stainless steels and further recrystallization behaviour. Previously Mehtonen et al. [10] reported that by lowering the deformation temperature, the stored energy of the material increased due to the less effective dynamic recovery, which further promotes static recrystallization at hot band annealing. The result is supported by this study, as high FRT and/or increased recrystallized fraction of the studied steels.

Tab.1 - Recrystallized fractions for the studied steels. (Note: in Channel5 analyses following parameters are used when determinate the recrystallization/recover/deform grain fractions. Minimum angle for low-angle grain boundary (LAGB) was set to 2.5° and minimum angle for high-angle grain boundary (HAGB) to 15°.)

RECRYSTALLIZED FRACTION						
material FRT-CT	Deformed [%]		Recovered [%]		Recrystallized [%]	
	subsurface	centreline	subsurface	centreline	subsurface	centreline
low-high	91.0	60.8	4.3	37.2	4.7	2.0
middle-high	68.2	49.9	19.1	45.8	12.7	4.4
high-high	50.8	20.9	29.7	72.3	19.5	6.8
low-low	86.6	23.4	7.9	74.0	5.6	2.6
middle-low	47.4	22.3	36.5	72.1	16.1	5.6
high-low	38.2	7.7	42.7	87.8	19.0	4.6

In order to analyse the evolution of grain size after hot rolling and coiling, the grain sizes of the steels were measured using EBSD data. Fig. 3 shows the grain size distribution of the studied steel samples. From the Fig. 3 it is seen that with increasing FRT low- and high-angle grain size increase both at the surfaces and centrelines, since e.g. at low and high FRT (and high CT) the grain sizes were 2.4 μm and 4.6 μm at the surface and 3.7 μm and 7.5 μm at the centreline, respectively. The increase in grain sizes is due to the re-crystallization following grain growth during hot rolling (see Table 1).

grain size decreases at both surfaces and centrelines, e.g. at high and low CT (low FRT) the grain size increase from 2.4 μm to 3.1 μm at the surface and from 3.7 μm to 6.3 μm at the centreline. The same trend was observed with the recrystallized fractions (Table 1) as the low CT increased the percentage of the recrystallized grains.

Opposite to FRT, with increasing CT the low and high angle

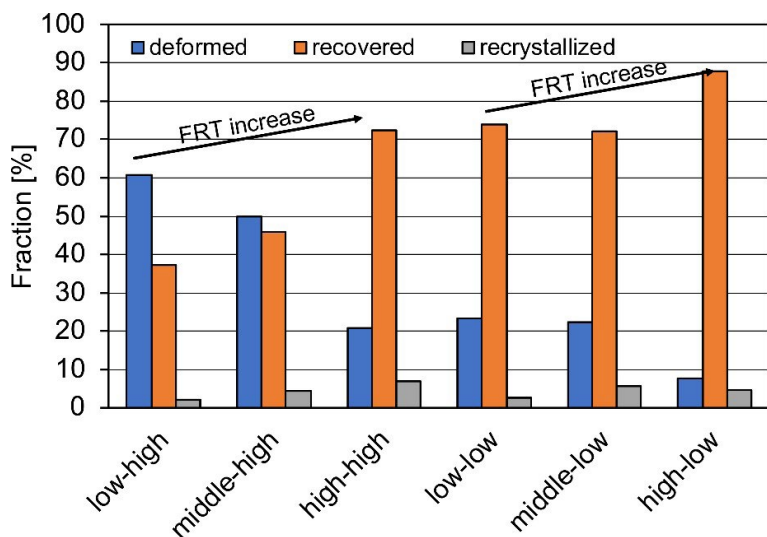


Fig.2 - Fraction of deformed, recovered and recrystallized structures of the investigated materials at the centreline.

Effective coarse grain size ($d_{90\%}$), i.e. grain size at 90 % in the cumulative grain size distribution, is showing the few biggest grains from the EBSD acquisition. $d_{90\%}$ value is showing, how homogenised grain size is distributed. In this case, it is behaviour similar to the high-angle grain

sizes when FRT is decreased. Typically, coarse grains effect on the mechanical properties such as impact energies. However, in this study mechanical properties were not determined.

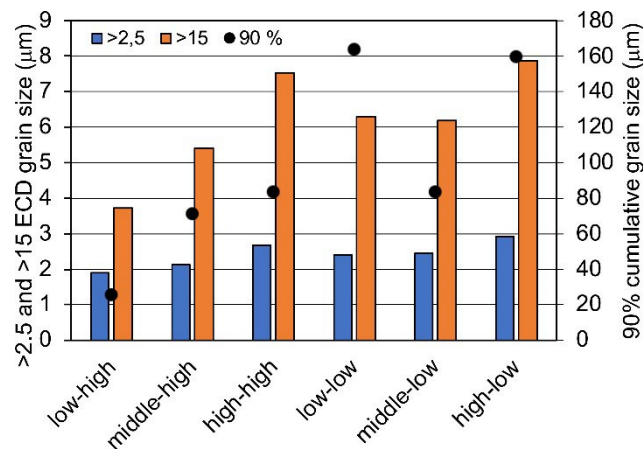
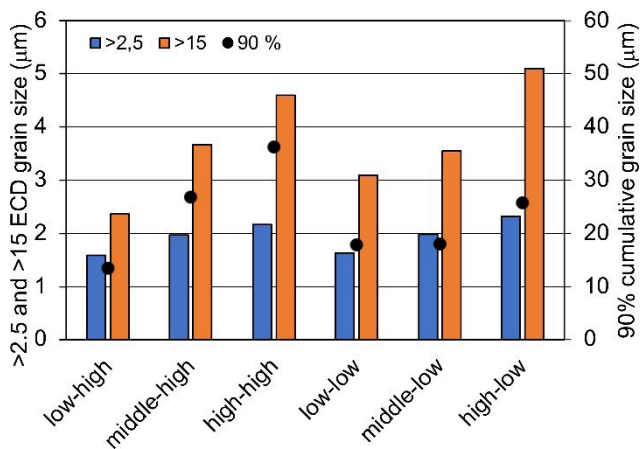


Fig.3 - Mean low- ($>2.5^\circ$) and high-angle (>15) equivalent circle diameter (ECD) grain sizes of the investigated materials at the surface (left) and centreline (right).

EBSD was also utilized to determine the microtexture of the studied steels. Fig. 4. presents the orientation distribution functions (ODFs) as $\phi_2=45^\circ$ cross-sections generally for ferritic stainless steels and Fig. 5 for the studied samples. It is evident that the texture varies through thickness. The subsurface texture is affected by the newly formed recrystallized grains together with elongated grains parallel to the rolling direction. At the surface, shear texture is dominant due to the shear deformation and the

main texture components are $\sim\{112\}<111>$, $\sim\{110\}<112>$, and $\sim\{011\}<110>$. Only slight variation in the individual maxima along the texture fibres were observed with the variation of FRT. However, the high CT sharpened the Goss texture as maximum texture intensity changes for the investigated samples were 6 – 12, 10 – 15, and 5 – 12 for the low, middle, and high FRTs. A decrease in FRT and CT strengthens the texture intensities at the subsurface.

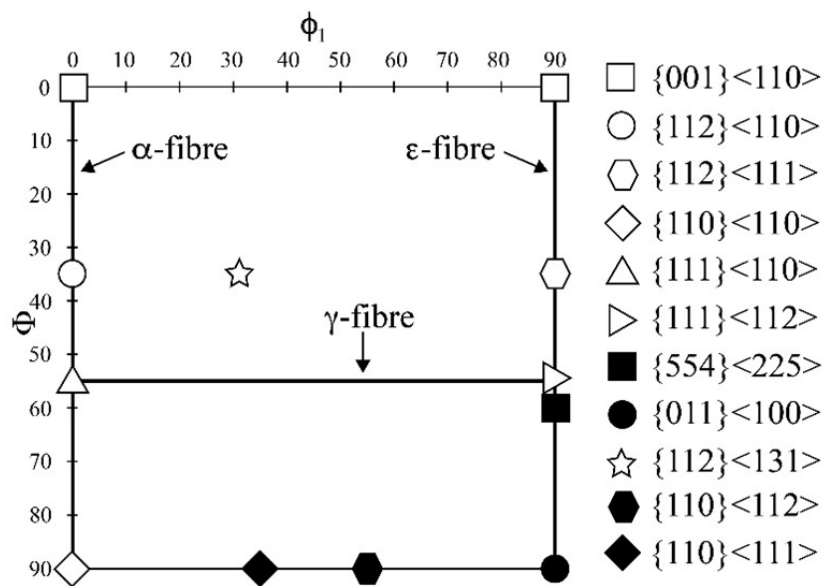


Fig.4 - Alpha, gamma, and epsilon fibres and the important texture components of the BBC structure in the $\Phi_2=45^\circ$ section.

Plane strain deformation and dynamic recovery are present at the centreline. Hence, the sharp α -fibre is evident with the sharp texture components of $\sim\{001\}<110>$ and $\sim\{112\}<110>$. The highest texture intensity maximum are 11, 11, and 9 for the low, middle, and high FRT samples with the low CT. With high CT, the texture gradients decrease, except in the low FRT sample. According to the microstructural characterization of the low-high sample, the grains seemed to be the most pancaked due to the less dynamic recovery. It could be assumed that this would result in a strong texture. Gao et al. [12] reported that the decrease in the hot deformation temperature shifted the orientation maximum from $\sim\{001\}<110>$ towards $\sim\{111\}<110>$ due to an increase in the lattice rotations, which promoted the development of texture towards stable end orientations. In the current study, the orientation maximum were shifted from $\sim\{001\}<110>$ towards $\sim\{111\}<110>$ by decreasing FRT or CT. However, the differences were not that significant. Low FRT and/or CT increase intensity towards $\sim\{112\}<110>$ texture component, which is known to increase grain rotations and texture towards $\sim\{112\}<110>$ component from $\sim\{001\}<110>$ component enhancing good formability of the final product [11].

At the centreline, in the γ -fibre the texture component

of $\sim\{554\}<225>$ was detected. The intensity maximum increases as FRT increases or CT decreases. Also, a sharp α -fibre texture component of $\sim\{001\}<110>$ is observed for the low-low or low-high sample, being weaker for other studied samples. The sharp texture may be due to the microstructure as discussed previously. Generally, at the centreline, lower finish rolling and coiling temperatures sharpened the α - and γ -fibres and texture.

A sharp γ -fibre texture component of $\sim\{001\}<110>$ is detected especially for low FRT specimens. In the further processing, the presence of $\sim\{001\}<110>$ orientated grains are challenging since their pronounced tendency to recover instead of recrystallizing. In addition, grains with $\sim\{001\}<110>$ orientation are last to recrystallize and the process is time-consuming. To obtain excellent properties of the final product, these orientations should be avoided.

Generally, the intensity of the γ -fibre texture correlates with the normal r-value since good formability requires γ -fibre texture. Hence, by increasing the in-grain shear band content and optimum texture components the hot band structure will recrystallize after further processing. This kind of structure can be achieved by enhancing the formation of {111} oriented grains, i.e. decreasing the FRT.

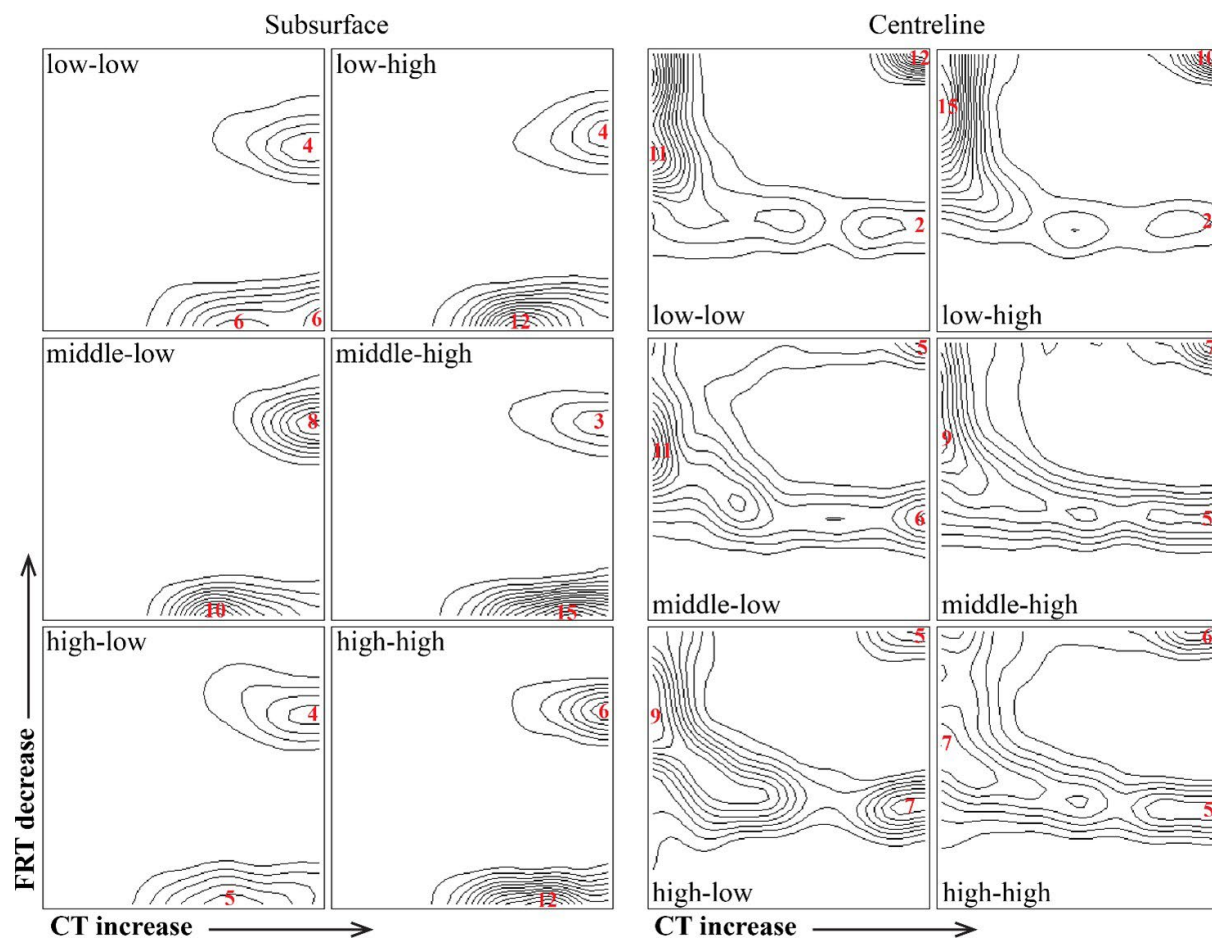


Fig.5 - $\phi_2=45^\circ$ sections of ODFs at the surface (left) and centreline (right) positions in investigated samples.

SUMMARY

The effect of hot rolling and coiling temperature on microstructure and texture of stabilized high-Cr ferritic stainless steel was investigated. The finish hot rolling temperature varied from low, middle to high and the coiling temperature from low to high. The resultant microstructures, grain sizes, and textures were examined using EBSD. It turned out that by lowering the FRT the stored energy of the material increased by means of deformed and/or recovered grains. This would enhance the static recrystallization in further hot band annealing as the stored energy of the material is increased since dynamic recovery during hot rolling decreased. A sharp α -fibre texture component of $\sim\{001\}<110>$ is detected especially for low FRT specimens. By decreasing FRT or CT, the orientation maximums were shifted from $\sim\{001\}<110>$ towards $\sim\{111\}<110>$. Hence, in order to obtain the preferred orientations, lower FRT and/or CT are recommended.

ACKNOWLEDGMENTS

Financial assistance of the Business Finland, project TO-CANEM – Towards Carbon-neutral Metals, is acknowledged.

REFERENCES

- [1] Yazawa Y, Ishii K, Okada S, Ujiro T, Yamasita H. Ni Mo-Free Stainless Steel with High Corrosion Resistance. *Corrosion Engineering*. 2007;56(10):599-606.
- [2] Hua M, Garcia C, DeArdo AJ, Tither G. Dual-stabilized ferritic stainless steels for demanding applications such as automotive exhaust systems. *Iron and Steelmaker*. 1997;24(4):41-44.
- [3] Charles J, Mithieux JD, Santacreu PO, Peguet L. The ferritic stainless steel family: the appropriate answer to nickel volatility? 6th European Stainless Steel Conference Science and Market. 2008 June 10-13; Helsinki, Finland. p. 703-720
- [4] Chao HC. The mechanism of ridging in ferritic stainless steels. *Trans. ASM*. 1967;60(1):37-50.
- [5] Shin HJ, An JK, Park SH, Lee DN. The effect of texture on ridging of ferritic stainless steel. *Acta Materialia*. 2003;51(16):4693-4706. Available from: [https://doi.org/10.1016/S1359-6454\(03\)00187-3](https://doi.org/10.1016/S1359-6454(03)00187-3)
- [6] Raabe D, Lücke K. Influence of particles on recrystallization textures of ferritic stainless steels. *Steel Research*. 1992;63(10):457-464. Available from: <https://doi.org/10.1002/srin.199201742>
- [7] Raabe D. Experimental investigation and simulation of crystallographic rolling textures of Fe-11Cr steel. *Materials Science and Technology*. 1995;11(10):985-993. Available from: <https://doi.org/10.1179/mst.1995.11.10.985>
- [8] Raabe D, Lücke K. Textures of ferritic stainless steels. *Materials Science and Technology*. 1993;9(4):302-312. Available from: DOI: [10.1179/mst.1993.9.4.302](https://doi.org/10.1179/mst.1993.9.4.302)
- [9] Yazawa Y, Muraki M, Kato Y, Furukimi O. Effect of chromium content on relationship between r-value and {111} recrystallization texture in ferritic steel. *ISIJ International*. 2003;43(10):1647-1651. Available from: <https://doi.org/10.2355/isijinternational.43.1647>
- [10] Mehtonen S, Palmiere E, Misra D, Karjalainen P, Porter D. Microstructural and texture development during multi-pass hot deformation of a stabilized high chromium ferritic stainless steel. *ISIJ International*. 2014;54(6):1406-1415. Available from: <https://doi.org/10.2355/isijinternational.54.1406>
- [11] Kodukula S. Ridging in stabilized ferritic stainless steels. The effects of casting and hot-rolling parameters. Doctoral Dissertation. Oulu: University of Oulu; 2012. 134 p. Available from: <http://urn.fi/urn:isbn:9789526231259>
- [12] Gao F, Liu Z, Liu H, Wang G. Influence of the finish rolling temperatures on the microstructure and texture evolution in the ferritic stainless steels. *Acta Metallurgica Sinica (English Letters)*. 2011;24(5):343-350.

TORNA ALL'INDICE >